

Finite momentum superconductivity in superconducting hybrids: Orbital mechanism

M. Yu. Levichev,¹ I. Yu. Pashenkin,¹ N. S. Gusev,¹ and D.Yu. Vodolazov^{1,*}

¹*Institute for Physics of Microstructures, Russian Academy of Sciences, 603950, Nizhny Novgorod, GSP-105, Russia*
(Dated: September 27, 2023)

Normally in superconductors, as in conductors, in the state with zero current I the momentum of superconducting electrons $\hbar q = 0$. Here we demonstrate theoretically and present experimental evidences that in superconducting/normal metal (SN) hybrid strip placed in in-plane magnetic field B_{in} finite momentum state ($\hbar q \neq 0$) is realized when $I = 0$. This state is characterized by current-momentum dependence $I(q) \neq -I(-q)$, nonreciprocal kinetic inductance $L_k(I) \neq L_k(-I)$ and different values of depairing currents I_{dep}^{\pm} , flowing along the SN strip in opposite directions. Found properties have *orbital* nature and are originated from gradient of density of superconducting electrons ∇n across the thickness of SN strip and field induced Meissner currents. We argue that this type of finite momentum state should be rather general phenomena in superconducting structures with artificial or intrinsic inhomogeneities.

PACS numbers:

I. INTRODUCTION

Normally in superconductors, also as in normal conductors (metals or semiconductors) the state with zero total current $I = 0$ is characterized by zero momentum $\hbar q = 0$ of superconducting electrons ($q = \nabla\phi + 2\pi A/\Phi_0$, where ϕ is a phase of superconducting order parameter, A is a vector potential and $\Phi_0 = \pi\hbar c/|e|$ is magnetic flux quantum). Such an *ordinary* superconductor has antisymmetric current-momentum dependence $I(q) = -I(-q)$ and symmetric kinetic inductance $L_k(I) = L_k(-I)$ (see Fig. 1(a,d)). Kinetic inductance $L_k \sim -dq/dI$ is a measure of inertia of superconducting electrons possessing the kinetic energy $E_k \sim \int n\hbar^2 q^2/(2m)dV \sim \int L_k(I)IdI$ (m is a mass of superconducting electrons, n is their density and V is a volume of superconductor). In superconductors L_k contributes to total inductance $L = L_k + L_g$, where L_g is ordinary (geometric) inductance, which does not depend on I .

However it has been predicted $q \neq 0$ despite of $I = 0$ for some superconducting systems. The most familiar examples are the ferromagnetic superconductor with magnetic exchange energy of order of superconducting gap Δ and thin superconducting strip placed in large in-plane magnetic field $\mu_B B_{in} \sim \Delta$. In these systems superconducting pairing occurs with finite center-of-mass momentum of electrons q_{FF} as it has been shown by Fulde and Ferrell¹ due to Zeeman splitting of energy of electrons having opposite spin. Recently, the similar Fulde-Ferrell (FF) state has been found theoretically in superconductor/ferromagnet (SF)^{2,3}, superconductor/ferromagnet/normal metal (SFN)⁴ and nonequilibrium SN hybrids⁵⁻⁷. In these hybrid superconductors there are local nonzero currents flowing in opposite directions in different layers which distinguishes it from the original FF state. Both cases we call here as FF state/superconductor. FF superconducting strip at $I = 0$ has two degenerate states with $q = \pm q_{FF}$ due to finite size effect⁸ (for infinite sample q_{FF} may have any direc-

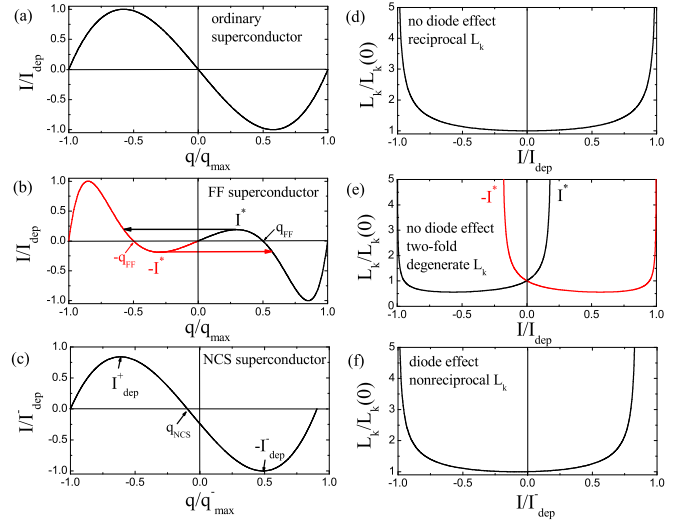


FIG. 1: Current-momentum dependence in ordinary (panel a), Fulde-Ferrell (b) and noncentrosymmetric (c) thin and narrow superconducting strip with uniform current distribution over the width of superconductor. In FF strip $I(q) = -I(-q)$ (as in ordinary superconductor) and there are two degenerate finite momentum states ($\pm q_{FF}$) while in NCS strip $I(q) \neq -I(-q)$ and there is one finite momentum state with $q = q_{NCS}$. In panels (d-e) we present corresponding dependencies of kinetic inductance $L_k(I) \sim -dq/dI$. In NCS superconductor $L_k(I) \neq L_k(-I)$ which is a fingerprint of this state, also as the diode effect ($I_{dep}^- \neq I_{dep}^+$). In ordinary and FF superconductors $I_{dep}^- = I_{dep}^+$, while $L_k(I)$ is two fold degenerate in FF superconductor in current range $-I^* < I < I^*$.

tion) and antisymmetric $I(q) = -I(-q)$ dependence^{8,9} (see Fig. 1(b)). At small currents $-I^* < I < I^*$ this system has two stable states⁹ which have different values of kinetic inductance L_k ¹⁰ - see Fig. 1(e). Depairing current in FF superconductor does not depend on current direction which reflects absence of particular direction for q_{FF} . As current increases and approaches to $\pm I^*$ (see Fig. 1(b)) FF superconductor switches to the state

having opposite q_{FF} at $I = 0$. If during this transition FF superconductor is not heated considerably it stays in superconducting state⁸.

Besides that there is another class of superconducting materials where finite momentum superconductivity may exist. These are so called noncentrosymmetric (NCS) superconductors with no inversion center and where in presence of spin-orbit coupling and in-plane magnetic field finite momentum of superconducting electrons q_{NCS} with *particular* direction appears^{11–13}. It has been discussed recently that such a NCS superconductor should have different depairing (critical) currents flowing either in parallel or antiparallel to \vec{q}_{NCS} ^{14–16} and nonreciprocal kinetic inductance $L_k(I) \neq L_k(-I)$ ¹⁷ following from the current-momentum dependence $I(q) \neq -I(-q)$ (see Fig. 1(c,f)). Difference between critical currents means that ac current with an amplitude between these critical values should produce in NCS superconductor voltage of only one sign. This is the reason why the difference between critical currents is called as a superconducting diode effect (SDE).

In our work we present theoretical and experimental results which demonstrate that finite momentum superconductivity (FMS), typical for discussed above noncentrosymmetric superconductors, is realized in the superconductor/normal metal hybrid *without* spin-orbit coupling in presence of in-plane magnetic field (see Fig. 2(a)). In SN bilayer there is a thickness dependent 'density' of superconducting electrons $n(z)$ which is a coefficient between superconducting current density and momentum: $j(z) \sim -|e|n(z)q(z)$. In N layer finite n appears due to proximity induced superconductivity, and usually it is smaller than in S layer (this case is shown in Fig. 2(b)). In-plane magnetic field induces Meissner currents $j(z)$ and superconducting electrons possess momentum $q(z)$. For thin SN bilayer with thickness $d_S + d_N \ll \lambda$ ($\lambda \sim n^{-1/2}$ is a London penetration depth) one may neglect magnetic field arising from the Meissner currents and choose $\mathbf{A} = (B_{in}z, 0, 0)$ where $-(d_S + d_N)/2 < z < (d_S + d_N)/2$. In case $n(z) = const$ the total current $I \sim \int j(z)dz = 0$ when the *thickness averaged momentum* $q_0 = \int qdz/(d_S + d_N) = \nabla\phi = 0$. But in case $\nabla n(z) \neq 0$ one needs finite $q_0 = q_{NCS}$ to have $I = 0$. It describes the *orbital* mechanism of finite momentum superconductivity in SN strip. From mathematical point of view presence of both thickness averaged ∇n and B_{in} breaks the symmetry in SN strip and vector $\nabla n \times B_{in}$ defines the particular direction and value of q_{NCS} .

From above consideration it is clear that finite momentum state of this type has to exist in any superconductor having finite ∇n and B_{in} . Here we prove it for SN bilayer where S layer is a dirty superconductor with large resistivity (small diffusion coefficient D_S) in the normal state and N layer is a low-resistive normal metal having large diffusion coefficient $D_N \gg D_S$. In this system due to noticeable contribution of proximity induced superconductivity in N layer to total L_k we expect to have large

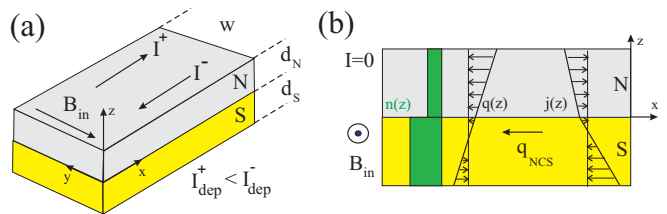


FIG. 2: (a) SN strip with transport currents of different directions placed in the in-plane magnetic field. (b) Sketch of thickness dependent 'density' of superconducting electrons $n(z)$, momentum $q(z)$ and superconducting current density $j(z) \sim -|e|n(z)q(z)$ in SN strip. For shown $n(z)$ and direction of B_{in} finite momentum q_{NCS} points against axis x .

difference between $L_k(I)$ and $L_k(-I)$ which is easy to observe experimentally and which is a fingerprint of FMS. This system also has diode effect, as it has been found earlier in Ref.¹⁸ but its relation with FMS was not discussed there. Another motivation to study this system comes from recent experiments where diode effect was observed in somewhere similar superconducting hybrids in presence of in-plane magnetic field^{17,19–22} and where we also expect contribution of the orbital mechanism to SDE.

The structure of our paper is following. In section II we present our theoretical results with characteristics of FMS which has an orbital mechanism in SN bilayer. In section IIIA we describe used experimental methods to study FMS in SN bilayer. In sections IIIB,C we present experimental results which demonstrate that we have finite momentum state in our superconducting hybrid and some unexpected its properties. In section IV we discuss that orbital mechanism of FMS has distinctive thickness dependence (it can be used to distinguish it from the mechanism connected with spin-orbit coupling) and our SN hybrid has expected behavior. In the same section we discuss other experiments on FMS and diode effect and its relation with our results. In section V we make conclusions.

II. THEORETICAL RESULTS

We start with presentation of our theoretical results. In Fig. 3 we show calculated $I(q_0, B_{in})$ and $L_k(I, B_{in})$ for the SN strip having following parameters: $d_S = d_N = 4\xi_c$ ($\xi_c = (\hbar D_S/k_B T_{c0})^{1/2}$, T_{c0} is a critical temperature of S layer) and ratio $D_N/D_S = 100$. To find it we use Usadel model (details of calculations are present in Appendix A). We choose two temperatures $T = 0.2$ and $T = 0.6T_{c0}$ which correspond to different physical situations. At $T = 0.2T_{c0}$ contribution of N layer is dominant in L_k at small fields and currents while at $T = 0.6T_{c0}$ N layer contributes much smaller in transport properties. In both cases finite field-controlled q_{NCS} appears (see upper insets in panels (a,b) of Fig. 3) leading to asymmetry of $I(q_0)$ and nonreciprocal $L_k(I)$. At $T = 0.2T_{c0}$ and

small B_{in} $q_{NCS} > 0$ because n is larger in N layer (in Fig. 2 opposite situation is shown, which is true for our SN strip at $T = 0.6T_{c0}$ at any I and B_{in}). At large B_{in} and currents close to I_{dep}^{\pm} superconductivity in N layer becomes suppressed and L_k increases. Transition between the states with different L_k is accompanied by appearance of the peak in dependencies $L_k(I)$ and $L_k(B_{in})$ - see Fig. 3(c,d). Note that this peak is absent in ordinary superconductors (see Fig. 1(d)) and/or much less pronounced in SN bilayers with small contribution of N layer to transport properties (see panel (d) in Fig. 3).

In the finite momentum state there is a difference between positive and negative depairing currents (see bottom insets in panels (a,b) of Fig. 3). I_{dep}^- is larger than I_{dep}^+ because current induced momentum partially compensate field induced momentum in N layer leading to recovery of proximity induced superconductivity. At small B_{in} it provides even increase of I_{dep}^- - the physically similar increase of I_c is realized in superconducting strip with nonequivalent edges being in out-of-plane magnetic field²³.

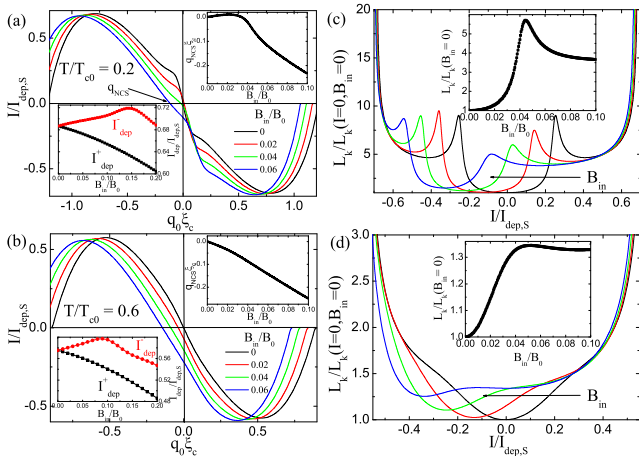


FIG. 3: Theoretical dependencies of current on momentum (a,b) and kinetic inductance on current (c,d) in SN bilayer at different in-plane magnetic fields and two temperatures $T = 0.2$ and $0.6T_{c0}$. In insets of panels (a,b) we present field dependencies of I_{dep}^{\pm} and finite momentum q_{NCS} at $I = 0$. In insets of panels (c,d) we show calculated field dependence of L_k in zero current state. Here $B_0 = \Phi_0/2\pi\xi_c^2$ and $I_{dep,S}$ is a depairing current of single S layer with thickness d_S .

III. EXPERIMENT

A. Methods

Experiment has been made with MoN/Cu strips. MoN is a dirty superconductor with resistivity in the normal state $\rho = 150\mu\text{Ohm} \cdot \text{cm}$ while Cu is low resistive metal (40 nm thick Cu has $\rho = 2.4\mu\text{Ohm} \cdot \text{cm}$ at $T=10$ K). The MoN/Cu bilayers are grown by magnetron sputter-

ing with a base vacuum level of the order of $1.5 \cdot 10^{-7}$ mbar on standard silicon substrates without removing the oxide layer and at room temperature. At first Mo is deposited in an atmosphere of a gas mixture Ar : $N_2 = 10 : 1$ at a pressure of $1 \cdot 10^{-3}$ mbar and then Cu is deposited in an argon atmosphere at a pressure of $1 \cdot 10^{-3}$ mbar. Finally, MoN/Cu strips has been made with help of mask free optical lithography.

Majority of measurements are done for thick $d_{MoN} = 40\text{nm}$, $d_{Cu} = 40\text{nm}$ samples. Altogether we have four long strips A1-A4 (width $4\mu\text{m}$, length 3mm) and several short bridges B1-B9 (width $4\mu\text{m}$, length $100\mu\text{m}$). All measured samples (A1-A2,A4, B2-B3) have nearly the same sheet resistance $R_s(300\text{K}) = 1\Omega$ and $R_s(T = 10\text{K}) = 0.6\Omega$ (variation from sample to sample is less than 10%) and critical temperature $T_c = 7.87\text{K}$ defined from condition that resistance $R(T_c) = 0.5R(10\text{K})$.

In addition we have made and studied two times thinner (MoN(20nm)/Cu(20nm)) reference long strips with the same width and length as thicker MoN/Cu strips to check the thickness dependence of the finite momentum state and verify its orbital nature. Their characteristics are present in Appendix C.

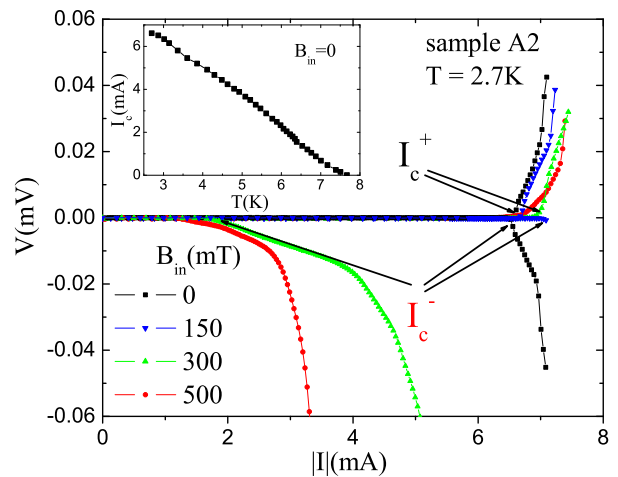


FIG. 4: Current-voltage characteristics of sample A2 at different B_{in} and $T = 2.7\text{K}$ (negative voltage corresponds to negative current while in x axis we show absolute value of the current), arrows indicate I_c^{\pm} . In the last points of IV curves there is jump to the normal state (not shown here). IV curves are not hysteretic before transition to the normal state. Critical currents (their absolute values) are determined from condition $|V|(I = I_c^{\pm}) = 0.5\mu\text{V}$. After transition to the normal state sample returns to the superconducting state at $I_r \simeq 1.6\text{mA}$ (when $I_c^{\pm} > I_r$) which practically does not depend on magnetic field and current direction. In inset we show temperature dependence $I_c(T)$ at $B_{in} = 0$.

Current voltage characteristics has been measured by four-probe method. Examples of IV curves are shown in Fig. 4 for sample A2 (in inset we present temperature dependence of I_c at $B_{in} = 0$). From these measurements we extracted critical currents I_c^{\pm} (see arrows in Fig. 4)

as function of B_{in} .

Impedance $Z = Z_{re} + iZ_{im}$ of MoN/Cu strip has been measured using Stanford Research SR830 lock-in amplifier. For measurements the four-probe method was used. Excitation signal with frequency $\nu = 100kHz$ and voltage 50mV from SR830 internal generator was supplied through 1 k Ω resistor. Signal from the sample is applied to the differential input of the SR830 through central electrodes of two coaxial cables. These measurements allow us to find field and current dependence of inductance $L = Z_{im}/2\pi\nu$. The same device has been used to measure first (R_ω) and second ($R_{2\omega}$) harmonic signals of the ac resistance at frequency of 130 Hz.

In our strips we have noticeable contribution of geometric inductance L_g to the total inductance. Using expression below for the strip with length l , width w and thickness d in limit $l \gg (w + d)^{24}$

$$L_g = \frac{\mu_0 l}{2\pi} \left(\ln \left(\frac{2l}{w+d} \right) + 1/2 \right) \quad (1)$$

we find for our long strips $L_g \simeq 4.7nH$.

B. Results below T_c

In Fig. 5 (see also Fig. 8 in Appendix B) we present $L_k(I)$ at different B_{in} and $I_c \pm(B_{in})$ at two temperatures 4.6 and 2.7 K which roughly corresponds to two temperatures present in Fig. 3. The main result is that in-plane field inductance L is nonreciprocal and it is the *main* proof that MoN/Cu strip has finite momentum at $I = 0$. Although we know $L(I, B_{in})$ it does not allow us to find q_{NCS} and its dependence on magnetic field - for that one has to know additionally $I(q_0)$ at least at one value of q_0 .

Experimental dependence $L(B_{in})$ at zero current and evolution of $L(I)$ with increase of B_{in} follow theoretical prediction at all magnetic fields with the important difference, for following discussion of diode effect, that in the experiment we do not reach the depairing current I_{dep}^\pm where theoretical L_k diverges (compare Figs. 5(a,b) with Figs. 3(c,d)). It occurs probably due to presence of edge defects which allow entry of *out-of-plane* vortices at $I < I_{dep}^\pm$ and it does not allow us to approach the depairing current. Indeed, image of the similar Cu/MoN strip made with help of electron microscope (see for example Fig. 1 in²⁵) shows that we have edge roughnesses with size of about 100 nm. Idea about vortex entry at $I > I_c^\pm$ is supported by experimental IV curves (see Fig. 4) - above the critical current SN strip transits to low resistive state which resembles flux flow regime.

In contrast to inductance our experimental results on superconducting diode effect are controversial. We find the sample-dependent difference between I_c^+ and I_c^- (in contrast to almost not sample-dependent $L(I, B_{in})$) and besides it has unexpected value and sign at relatively

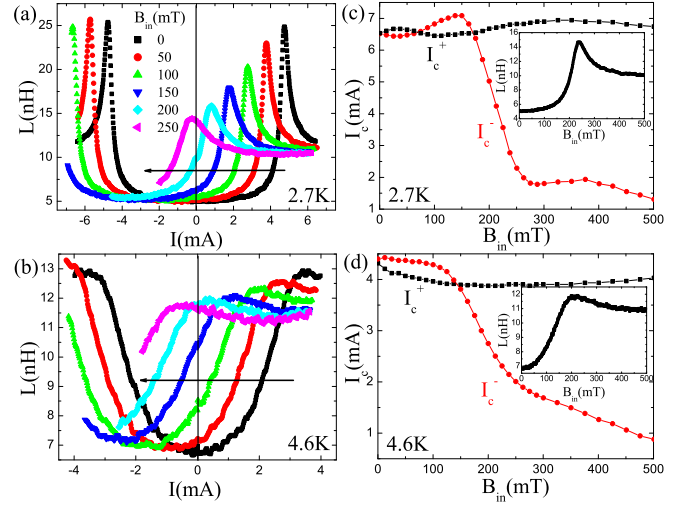


FIG. 5: Panels (a,b) - evolution of current dependent inductance of MoN/Cu strip (sample A2) in superconducting state with increase of in-plane magnetic field at $T=2.7K$ and $T=4.6K$, respectively. In panels (c,d) we present field dependent critical current and field dependent inductance at $I = 0$.

large B_{in} for all studied samples (compare Figs. 3, 5, 8 and 9). At magnetic field $B_{in} \lesssim 150mT$ the sign and value of SDE mainly coincide with prediction of our theory for samples A1, A4, B4 while for samples A2, B3 there is a sign change of diode effect with increase of B_{in} . At $B_{in} \gtrsim 150mT$ we have $I_c^- \ll I_c^+$ for all samples. The large difference (ratio $\eta = 2|I_c^- - I_c^+|/(I_c^- + I_c^+) > 1$) and its 'wrong' sign cannot be explained by our theory which predicts $I_c^- = I_{dep}^- \gtrsim I_c^+ = I_{dep}^+$.

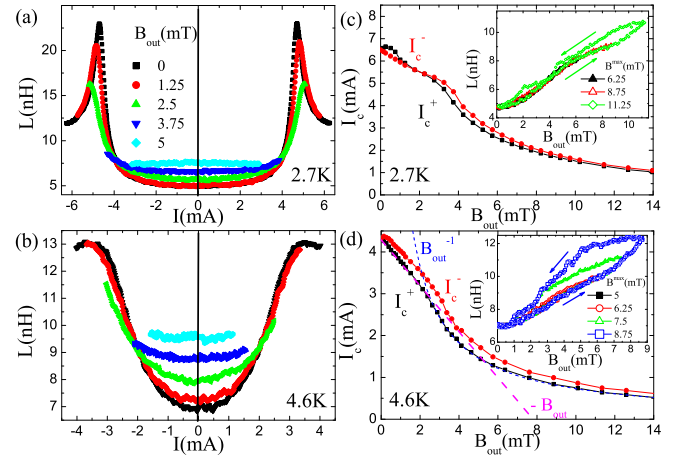


FIG. 6: Panels (a,b) - evolution of current dependent inductance of MoN/Cu strip (sample A2) with increase of out-of-plane magnetic field at $T=2.7K$ and $T=4.6K$, respectively. In panels (c,d) we present field dependent critical currents and inductance. Dependence $L(B_{out})$ for sweeping up and down field is hysteretic for relatively large amplitude of B_{out} which we relate with trapped out-of-plane vortices due to edge barrier for vortex entry/exit.

It could be supposed that in our experiment together with in-plane field there is small out-of-plane field B_{out} (due to not perfect alignment of the sample holder along superconducting coil which is a source of our magnetic field). Even small B_{out} , in comparison with B_{in} , strongly suppresses I_c and in presence of edge defects may lead to SDE which also has an orbital nature because it originates from the combined effect of Meissner and transport currents²³. Experimentally it was found in different superconductors²⁵⁻³⁰. Note, that probably the same mechanism is responsible for SDE observed in NbSe₂ bridge³¹ which follows from its sample-dependent character and nearly linear decay of I_c at small fields $\lesssim \Phi_0/2\pi\xi w$ which points out on the edge barrier controlled I_c^{\pm} ³². In the strip/bridge with edge defect strength of this type of SDE is controlled by parameters of the defect and η may be larger than unity as it follows from Ref.²⁵ which resembles our result at large B_{in} .

Therefore we measured $L(I, B_{out})$ and $I_c^{\pm}(B_{out})$ - see Fig. 6. Influence of bulk pinning in our hybrid is negligible, at least in used field range, as it follows from the typical for edge-barrier controlled field-dependent $I_c^{\pm}(B_{out})$ ³² (I_c^{\pm} drops nearly linearly at low fields and $I_c^{\pm} \sim 1/B_{out}$ at large fields - see panel (d) in Fig. 6). We find nearly reciprocal $L(I)$ while there is small superconducting diode effect, comparable in value with SDE at $B_{in} \lesssim 150mT$ and which also may change the sign (see Fig. 6(c)). The sign change does not follow from the model of Ref.²³ and in principle it may appear if there are defects on opposite edges of the strip with different magnetic field controlled 'strength' leading to different suppression of the edge barrier. The edge defects give nonreciprocal contribution to total L_k but on scale about of defect size (~ 100 nm) along the strip which is several orders of magnitude smaller than its length (3 mm). As a result it is difficult to observe nonreciprocal $L(I)$ in out-of-plane field.

From comparison of Fig. 5 and 6 we conclude that if even there is finite B_{out} in the experiment with in-plane field it cannot explain large difference between I_c^+ and I_c^- at $B_{in} \gtrsim 150mT$ because B_{out} suppresses them on equal foot. Besides at $B_{out} = 5mT$ ($I_c^{\pm}(5mT) \sim I_c^{\pm}(0)/2$) kinetic inductance practically does not depend on current, while in in-plane field L varies with current even at $B_{in} = 250mT$ ($I_c^-(250mT) \sim I_c^{\pm}(0)/3$). Therefore we exclude influence of B_{out} .

Sample-dependent $I_c^{\pm} < I_{dep}^{\pm}$ allows us to suppose that out-of-plane vortices enter the SN strip via local sample-dependent edge defects at $I > I_c^{\pm}$ and it launches the resistive state - on experimental IV curves there are vortex flow branches above I_c^{\pm} . At small fields, when the proximity induced superconductivity in Cu layer is slightly suppressed by B_{in} there is proportionality $I_c \sim I_{dep}$ (coefficient proportionality is sample-dependent). Because defect may have variation of its properties across the thickness of MoN/Cu strip at may lead to change the sign of diode effect, similar to one observed in out-of-plane field. Obviously our 1D model cannot catch this effect.

Large in-plane field stronger suppresses proximity induced superconductivity in Cu layer. Positive current suppresses it even more and we effectively have a single S layer with weak field dependence of I_c^+ at $B_{in} \lesssim \Phi_0/d_S^2 \sim 1300mT$ (at this or larger field we expect entry of in-plane vortices in S layer according to³³) which we observe in the experiment. Negative current partially recovers superconductivity in N layer (it is seen from decrease of experimental $L(I)$ at large B_{in}) and it may lead to appearance of in-plane vortices in N layer near SN interface at field $B_{in} \sim \Phi_0/(d_S + d_N)^2 \sim 320mT$ which is near our experimental value. In-plane vortices should favor entry of out-of-plane vortices and it may suppress the critical current and change the relation between I_c and I_{dep} . This is possible but speculative scenario. Theoretical description of out-of-plane vortex entry to SN strip with thickness dependent 'density' n , finite momentum q_0 and possible existence of row of in-plane vortices located on or close to SN interface is rather complicated 3D problem which needs separate study.

Single and multiple sign change of the diode effect with increase of in- or out-of-plane magnetic field were observed earlier in Refs.^{21,22,34,35} and predicted theoretically in^{15,36} for noncentrosymmetric superconductor. From that theories it follows that together with sign change of SDE there is strong change of $I(q)$ (see Fig. 5 in¹⁵ and Fig. 2 in³⁶) and, hence, $L_k(I)$. In our system we do not observe drastic variation of $L_k(I)$ when sign change of diode effect occurs and $L_k(I)$ evolves with increase of B_{in} as our theory predicts. In Refs.^{21,22,34,35} $L_k(I)$ has not been measured and it is difficult to interpret the origin of the effect.

C. Diode effect and nonreciprocal resistivity near T_c

By approaching to the critical temperature I_c^{\pm} decreases but still there is diode effect and $V(I) \neq -V(-I)$ - see Fig. 7. It is known that thermal fluctuations allow vortices (we keep in mind out-of-plane vortices) to enter the superconducting strip at the current less than I_c . The probability for vortex to overcome the edge barrier is proportional to Arrhenius factor $\exp(-dF(I)/k_B T)$ where $dF(I)$ is a current dependent height of the edge barrier which goes to zero at $I = I_c$ and it is proportional to the vortex energy at zero current $dF \sim F_0 = \Phi_0^2 d/16\pi^2 \lambda^{237-39}$. At $T \sim T_c$ both I_c and F_0 vanish which increases the impact of fluctuations. As a result near T_c the resistance R is finite even at $I \rightarrow 0$ and it could be nonreciprocal in case of different I_c^{\pm} because of $dF(I^+) \neq dF(I^-)$.

Additional mechanism which may contribute to nonreciprocal R is the current dependent viscosity of vortex motion. Indeed, the transport current with one direction stronger suppresses proximity induced superconductivity in N layer than the current with opposite direction which should affect the vortex velocity v and voltage $V \sim v$.

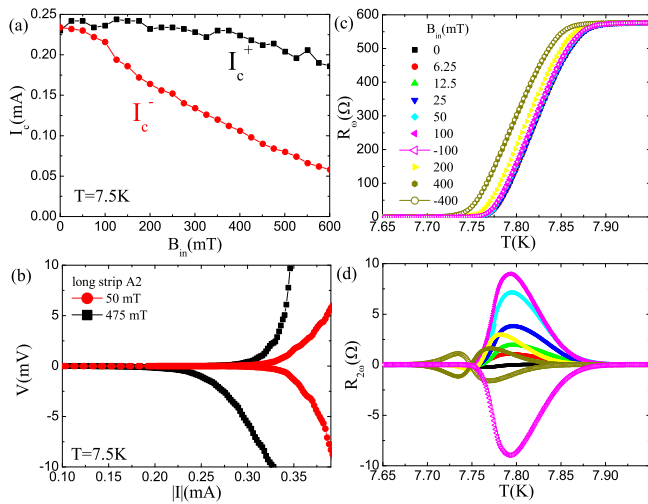


FIG. 7: Panel (a) - field dependent critical currents I_c^\pm of sample A2 at $T=7.5K$. Panel (b) - current voltage characteristics of strip A2 at different B_{in} . Panels (c,d) - temperature dependence of first and second harmonics of IV characteristics at different in-plane magnetic fields.

Our measurements of the first and second harmonics of IV characteristics confirm existence of nonreciprocal resistance at finite B_{in} near T_c (see panels c,d in Fig. 7).

Earlier finite $R_{2\omega}$ near T_c has been found for various hybrid superconducting structures placed in in-plane magnetic field where its origin has been related with spin-orbit coupling^{19,40–42}. Our experiment demonstrates existence of qualitatively similar result in MoN/Cu hybrid where we have orbital mechanism of finite momentum state, resulting in diode effect and nonreciprocal resistance near critical temperature. We believe that the same orbital mechanism has to exist in Ref.^{19,40–42} and compete with spin-orbit interaction.

IV. DISCUSSION

Proposed orbital mechanism of finite momentum state in hybrid superconductors is finite size (thickness) effect. We theoretically find that at relatively large B_{in} $q_{NCS} \sim -B_{in}(d_S + d_N)2\pi/\Phi_0$ for different thicknesses of S and N layers (for parameters of SN bilayer from Fig. 3 $q_{NCS} \simeq -B_{in}(d_S + d_N)2\pi/3\Phi_0$). It means that when the thickness of SN bilayer goes to zero $q_{NCS} \rightarrow 0$ at and orbital mechanism disappears (the same is valid when $d_N \rightarrow 0$). It gives the way to check its influence in the experiment - one may study thickness dependence of $L_k(I, B_{in})$ because for smaller thickness the larger B_{in} is needed to have the same q_{NCS} . Indeed, we find that for two times thinner sample MoN(20nm)/Cu(20nm) the change of $L(I)$ is less sensitive to B_{in} (compare Fig. 10(a) with Fig. 5(a,b)) than for thick strip which qualitatively coincide with our calculations (compare Fig. 3(b,d) with Fig. 10(c,d)).

Our experimental results indicate that one should be careful with interpretation of experiments on diode effect. We observe sign change of the diode effect with increase of magnetic field in two (one long and one short) thick samples and its absence in another two long and short thick samples at $B_{in} \lesssim 150mT$ while $L(I, B_{in})$ and, hence, $I(q)$ was almost the same for all long samples. It means that additional factor, having not intrinsic to given material character, may play a role. In our case we believe that sample-dependent edge defects are responsible for observed effect. In this respect measurements of $L_k(I, B_{in})$ give more reliable information about intrinsic origin of finite momentum state than measurements of $I_c^\pm(B_{in})$. Indeed, if there is strong variation of superconducting properties along the sample but on small distance it weakly affects the total kinetic inductance but it may strongly affect critical current because it is determined by the 'weakest' place.

At $B_{in} \gtrsim 150mT$ for all thick samples we find sign change of the diode effect and its considerably larger value in comparison with theoretical expectations. At the same time we do not observe any qualitative changes of $L(I)$. We believe that it could be connected with appearance of in-plane vortices in SN bilayer. If it is true it is also finite thickness effect and with decreasing the thickness of SN bilayer in-plane vortices (and sign change of diode effect) should appear at larger field. Somewhere similar effect appears in thin strip where we do not have sign change of diode effect at 2.7 K for all studied three samples up to $B_{in} = 500mT$ and at 4.6K it exists only for one sample.

In Ref.¹⁹ the diode effect was observed in multilayered Nb/V/Ta strip with thickness $d = 120nm$ and width $w = 50\mu m$. At low temperature SDE vanished which is in contrast to results of Refs.^{17,20–22} and our work where diode effect becomes more pronounced at low T. The width of Nb/V/Ta strip greatly exceeds effective Pearl magnetic field penetration depth λ^2/d except at $T \sim T_c$ (we assume that $\lambda(0) = 120nm$ as in dirty Nb because zero temperature coherence length $\xi(0) = 13nm$ of multilayer is close to ξ of dirty Nb). It means that current distribution is nonuniform over the width of Nb/V/Ta strip which automatically means that critical current has to be much smaller than the depairing current and resistive state is connected with entry and motion of out-of-plane vortices. The nonuniform current distribution may lead to vortex pinning at low temperature which destroys experimentally observed diode effect.

In Al/InGaAs/InAs/InGaAs heterostructures SDE was found and explained by the interplay between diamagnetic and external currents²², which qualitatively coincides with mechanism of the diode effect in SN bilayer proposed in Ref.¹⁸, here and in Ref.²³ for the superconducting strip with nonequivalent edges being in out-of-plane magnetic field. Assumption of authors of²² that different layers in heterostructure have different currents may be reformulated in terms of different densities of superconducting electrons and finite ∇n which has to lead

to finite q_{NCS} when there is in-plane magnetic field. In terms of Ref.²² we have strong coupling regime between S and N layers and in our case if in-plane vortices appear at large B_{in} they should be more like Abrikosov vortices than Josephson ones.

In Refs.^{17,20,21} SDE was observed in SNS Josephson junction (JJ) and, hence, our results cannot be applied directly to that systems. But all studied junctions have hybrid SN banks where in-plane magnetic field should produce FMS. There is a question, may finite q_{NCS} in the SN banks affects the transport properties of JJ even if in N weak link there is no ∇n or it is small? To answer this question one has to calculate transport properties of SN-N-SN junction taking into account finite thicknesses of SN banks and normal weak link which is difficult 2D problem. Therefore at the moment we cannot claim that the orbital mechanism is involved in diode effect observed in that works, although results from Refs.^{17,20,21} look qualitatively similar to our results.

V. CONCLUSION

We demonstrate appearance of finite momentum state in SN bilayer placed in in-plane magnetic field. Experimentally, presence of FMS is proven via observation of nonreciprocal inductance $L(I) \neq L(-I)$ in several MoN/Cu strips being in in-plane magnetic field. It has an orbital nature as it follows from the experiment with samples having different thickness and expected zero or negligible contribution of spin-orbit coupling in our system.

We also experimentally observe superconducting diode effect but in contrast to results with $L(I, B_{in})$ it has rather cumbersome sample-dependent behavior. We speculate that it could be connected with presence of the sample-dependent edge defects and appearance of in-plane vortices in large enough B_{in} .

Taking into account our results and discussion in Introduction we may claim that finite momentum state is not elusive or rear phenomena in superconducting structures. Any nonuniformities (material or geometric) lead to $\nabla n \neq 0$ and in presence of magnetic field the particular direction appears along which there is a difference in critical currents (SDE) and nonreciprocal L_k . If the diode effect originates from local edge defects (as in case of superconducting strip placed in out-of-plane field) it may not lead to noticeable nonreciprocal L_k of a whole sample due to local nature of FMS in this case.

Acknowledgments

The work is supported by the Russian Science Foundation (project No. 23-22-00203).

Appendix A: Model

To calculate transport properties (critical current, kinetic inductance) of SN bilayer we use the one-dimensional Usadel equation for normal g and anomalous f quasi-classical Green functions⁴³. With standard angle parametrization $g = \cos\Theta$ and $f = \sin\Theta \exp(i\varphi)$ the Usadel equations in different layers can be written as

$$\hbar D_S \frac{\partial^2 \Theta_S}{\partial z^2} - (\hbar \omega_k + D_S \hbar q^2 \cos \Theta_S) \sin \Theta_S + 2\Delta \cos \Theta_S = 0, \quad (\text{A1})$$

$$\hbar D_N \frac{\partial^2 \Theta_N}{\partial z^2} - (\hbar \omega_k + D_N \hbar q^2 \cos \Theta_N) \sin \Theta_N = 0, \quad (\text{A2})$$

where subscripts S and N refer to superconducting and normal layers, respectively. Here D is the diffusion coefficient for corresponding layer, $\hbar \omega_k = \pi k_B T (2k + 1)$ are the Matsubara frequencies (k is an integer number), $\hbar q = \hbar (\nabla \varphi + 2\pi \mathbf{A} / \Phi_0) = \hbar (q_0 + 2\pi \mathbf{A} / \Phi_0)$ is the momentum of Cooper pairs, φ is the phase of the order parameter, \mathbf{A} is the vector potential, $\Phi_0 = \pi \hbar c / |e|$ is the magnetic flux quantum. Δ is the superconducting order parameter, which satisfies to the self-consistency equation

$$\Delta \ln \left(\frac{T}{T_{c0}} \right) = 2\pi k_B T \sum_{\omega_k > 0} \left(\sin \Theta_S - \frac{\Delta}{\hbar \omega_k} \right), \quad (\text{A3})$$

where T_{c0} is the critical temperature of single S layer in the absence of magnetic field. These equations are supplemented by the Kupriyanov-Lukichev boundary conditions on SN interface⁴⁴

$$D_S \frac{d\Theta_S}{dz} = D_N \frac{d\Theta_N}{dz} \quad (\text{A4})$$

For simplicity we consider case with zero barrier between layers and continuous Θ on SN interface. For interfaces with vacuum we use the boundary condition $d\Theta/dz = 0$.

We assume that the thickness $d_S + d_N$ of SN strip is much smaller than the London penetration depth λ while the width w is smaller than the Pearl penetration depth $\Lambda = \lambda^2 / (d_S + d_N)$ which allows us to neglect the effect of superconducting screening on the vector potential and magnetic field. We choose vector potential $\mathbf{A} = (-B_{in}z, 0, 0)$ with thickness averaged $\int \mathbf{A} dz = 0$ (here $-(d_S + d_N)/2 < z < (d_S + d_N)/2$).

To calculate the current density j , 'density' of superconducting electrons n and current $I = w \int j dz$ we use the standard expression

$$j(z) = -\frac{2\pi k_B T}{|e|\rho} q(z) \sum_{\omega_k > 0} \sin^2 \Theta = -|e| n(z) q(z) \frac{\hbar}{m} \quad (\text{A5})$$

$$n(z) = \frac{m}{\hbar} \frac{2\pi k_B T}{e^2 \rho} \sum_{\omega_k > 0} \sin^2 \Theta = \frac{mc^2}{8\pi |e| \lambda^2(z)} \quad (\text{A6})$$

where $\rho = 2|e|D_{S,N}N(0)$ is the residual resistivity of the corresponding layer, $N(0)$ is density of states of electrons per one spin at the Fermi level in the normal state (we assume identical $N(0)$ in S and N layers) and m is a 'mass' of superconducting electrons.

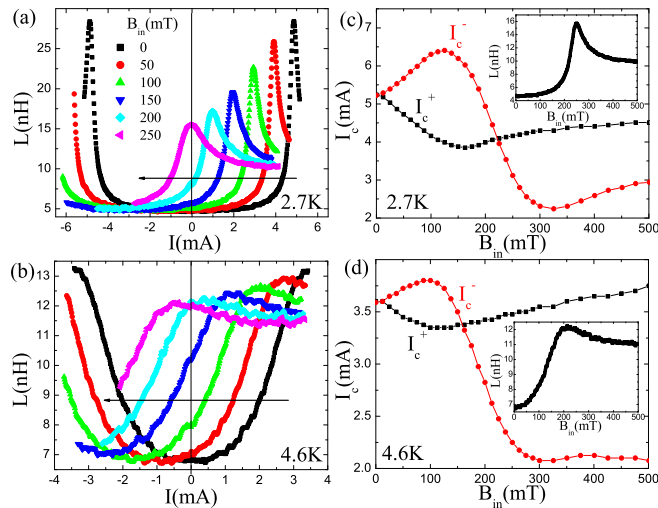


FIG. 8: Panels (a,b) - evolution of current dependent inductance of MoN/Cu strip (sample A4) with increase of in-plane magnetic field at $T=2.7K$ and $T=4.6K$, respectively. In panels (c,d) we present field dependent critical current and inductance.

Equations (A1-A3) are solved numerically by using iteration procedure. For initial distribution $\Delta(z) = const$ and chosen q_0 , B_{in} we solve Eqs. (A1,A2) (in numerical procedure we use Newton method combined with tridiagonal matrix algorithm). Found solution $\Theta(z)$ is inserted to Eq. (A3) to find $\Delta(z)$ and than iterations repeat until the relative change in $\Delta(z)$ between two iterations does not exceed 10^{-8} . Length is normalized in units of $\xi_c = \sqrt{\hbar D_S / k_B T_{c0}}$, energy is in units of $k_B T_{c0}$, current is in units of depairing current $I_{dep,S}$ of single S layer with the thickness d_S , the magnetic field is in units of $B_0 = \Phi_0 / 2\pi \xi_c^2$ (B_0 by factor 1.76 is smaller than the out-of plane second critical field $B_{c2}(T=0)$ of single S layer). Typical step grid in S and N layers is $\delta z = 0.1 \xi_c$. In calculations we used the following parameters: $d_S = d_N = 4\xi_c$, $D_N/D_S = 100$ for thick strip and $d_S = d_N = 2\xi_c$, $D_N/D_S = 80$, which are not far from experimental values.

With calculated $I(q_0)$ we find kinetic inductance per unit of length of the strip

$$L_k = -\hbar c^2 (dI/dq_0)^{-1} / 2|e| \quad (A7)$$

and I_{dep}^\pm as *absolute* value of maximal positive and negative superconducting currents where $dI/dq_0 = 0$.

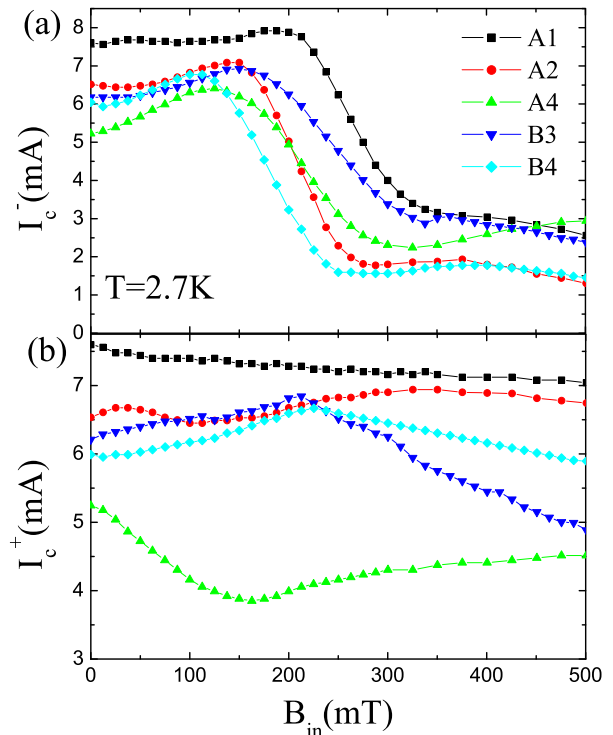


FIG. 9: Panels (a) and (b)- field dependent critical currents I_c^\pm for different MoN/Cu strips (A1, A2, A4 - long strips, B3, B4 - short strips) at $T = 2.7K$.

Appendix B: Results for different thick samples

In Fig. 8 we show $L(I, B_{in})$ and $I_c^\pm(B_{in})$ for strip A4. While dependence $L(I, B_{in})$ is rather close to one for strip A2 (the same is valid for sample A1 - results are not shown here) field dependencies of I_c^\pm are quantitatively different at $B_{in} \lesssim 150mT$ and $T = 2.7K$. We explain it by specific to each sample edge defects.

In Fig. 9 we show sample-dependent $I_c^\pm(B_{in})$ for all studied three long and two short strips at $T = 2.7K$. Despite of quantitative differences one may notice some general properties for all strips. At weak fields ($B_{in} \lesssim 150mT$) I_c^- slightly increases, which is in accordance with our theory. But than there is sharp decrease of I_c^- and it becomes much smaller than I_c^+ , which is opposite to our model. On contrary, critical current I_c^+ varies much weaker while its field dependence changes from strip to strip.

Appendix C: Results for thinner samples

In Fig. 10(a,b) we present results of transport measurements for two times thinner MoN/Cu long strips at $T = 4.6K$ (samples A1-A3, the width and length are the same as for thick long strips, $d_{MoN} = d_{Cu} = 20nm$,

$T_c = 7.37K$, 20 nm thick Cu has $\rho = 2.9\mu\Omega \cdot cm$ at $T=10$ K, resistivity of MoN layer is the same as for 40 nm thick layer). In Fig. 10 (c,d) we show theoretical results ($d_S = d_N = 2\xi_c$, $D_N/D_S = 80$, $T = 0.6T_{c0}$). Inductance is nonreciprocal in presence of in-plane field which is proof of appearance of finite momentum state but we need much larger field to have qualitatively the same change of L as for thick strip. From the experiment we conclude that our maximal accessible field ($B_{in} = 500mT$) does not destroy proximity induced superconductivity in Cu layer (at zero current) because we do not see a peak in dependence $L(B_{in})$ (see inset in Fig. 10 (b)). Qualitatively the same results are obtained at $T = 2.7K$ (not shown here). These findings prove that we have in the experiment orbital mechanism of finite momentum state.

Sign change of the diode effect is observed only in sample A1 (see Fig. 10(b)) at 4.6K and for all studied samples it does not exist at 2.7K (dependencies $I_c^\pm(B_{in})$ resemble ones for samples A2-A3 at $T = 4.6K$ with maximum of $I_c^-(B_{in})$ at $\sim 250mT$). In this respect results for thinner sample better follow our theoretical calculations with no sign change of the diode effect (see inset in Fig. 10(c)). However we cannot rule out its appearance at large fields where L should reach the peak in dependence $L(B_{in})$.

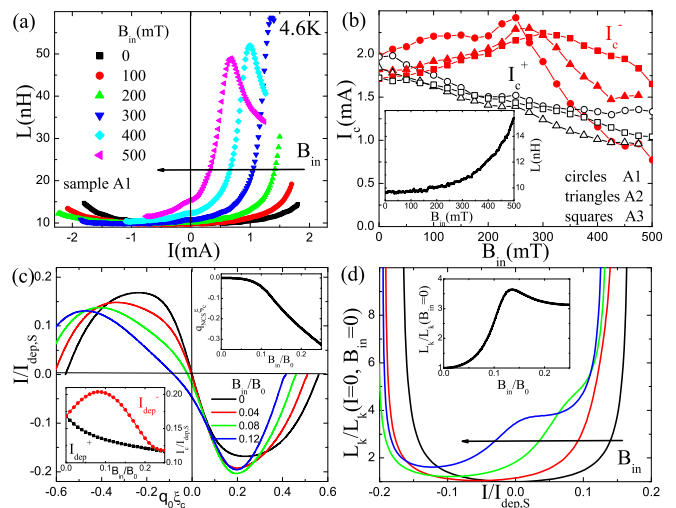


FIG. 10: Panel (a) - evolution of current dependent inductance of thin MoN(20nm)/Cu(20nm) strip (sample A1) with increase of in-plane magnetic field at $T=4.6K$. Panel (b) - field dependent positive and negative critical currents of strips A1-A3 at $T=4.6$ K. In panels (c,d) we present results of theoretical calculations for thin SN strip.

* Electronic address: vodolazov@ipmras.ru

- ¹ P. Fulde and R. A. Ferrell, Superconductivity in a strong spin-exchange field, Phys. Rev. **135**, A550 (1964).
- ² S. Mironov, A. Mel'nikov, and A. Buzdin, Vanishing Meissner effect as a Hallmark of in-Plane Fulde-Ferrell-Larkin-Ovchinnikov Instability in Superconductor-Ferromagnet Layered Systems, Phys. Rev. Lett. **109**, 237002 (2012).
- ³ A. M. Bobkov and I. V. Bobkova, Enhancing of the Critical Temperature of an In-Plane FFLO State in Heterostructures by the Orbital Effect of the Magnetic Field, JETP Letters, **99**, 333 (2014).
- ⁴ S. V. Mironov, D. Vodolazov, Yu. Yerin, A. V. Samokhvalov, A. S. Melnikov, and A. Buzdin, Temperature Controlled Fulde-Ferrell-Larkin-Ovchinnikov Instability in Superconductor-Ferromagnet Hybrids, Phys. Rev. Lett. **121**, 077002 (2018).
- ⁵ I. V. Bobkova and A. M. Bobkov, In-plane Fulde-Ferrell-Larkin-Ovchinnikov instability in a superconductor/normal metal bilayer system under nonequilibrium quasiparticle distribution, Phys. Rev. B **88**, 174502 (2013).
- ⁶ J. A. Ouassou, W. Belzig, and J. Linder, Prediction of a Paramagnetic Meissner Effect in Voltage-Biased Superconductor-Normal-Metal Bilayers, Phys. Rev. Lett., **124**, 047001 (2020).
- ⁷ M. Yu. Levichev, I. Yu. Pashenkin, N. S. Gusev, and D. Yu. Vodolazov, Voltage controllable superconducting state in the multiterminal superconductor-normal-metal bridge, Phys. Rev. B **103**, 174507 (2021).
- ⁸ V. D. Plastovets and D. Y. Vodolazov, Dynamics of Domain Walls in a Fulde-Ferrell Superconductor, JETP Lett. **109**, 729 (2019).

- ⁹ K. V. Samokhin, B. P. Truong, Current-carrying states in Fulde-Ferrell-Larkin-Ovchinnikov superconductors, Phys. Rev. B **96**, 214501 (2017).
- ¹⁰ P.M. Marychev and D.Y. Vodolazov, Extraordinary kinetic inductance of superconductor/ferromagnet/normal metal thin strip in an Fulde-Ferrell state, Journal of Physics, Condensed Matter **33**, 385301 (2021).
- ¹¹ V.M. Edelshtein, Characteristics of the Cooper pairing in two-dimensional noncentrosymmetric electron systems, Sov. Phys.-JETP **68**, 1244 (1989).
- ¹² D.F. Agterberg, Novel magnetic field effects in unconventional superconductors, Physica C **387**, 13 (2003).
- ¹³ Non-Centrosymmetric Superconductors, edited by E. Bauer and M. Sigrist (Springer, Berlin, 2012).
- ¹⁴ N. F. Q. Yuan and L. Fu, Supercurrent diode effect and finite-momentum superconductors, Proceedings of the National Academy of Sciences **119** (2022), 10.1073/pnas.2119548119.
- ¹⁵ A. Daido, Y. Ikeda, Y. Yanase, Intrinsic superconducting diode effect, Phys. Rev. Lett. **128**, 037001 (2022).
- ¹⁶ J. J. He, Y. Tanaka, N. Nagaosa, A phenomenological theory of superconductor diodes, New J. Phys. **24**, 053014 (2022).
- ¹⁷ C. Baumgartner, L. Fuchs, A. Costa, S. Reinhardt, S. Gronin, G. C. Gardner, T. Lindemann, M. J. Manfra, P. E. F. Junior, D. Kochan, J. Fabian, N. Paradiso, C. Strunk, Supercurrent rectification and magnetochiral effects in symmetric Josephson junctions, Nat. Nanotech. **17**, 39 (2022).
- ¹⁸ D. Yu. Vodolazov, A. Yu. Aladyshkin, E. E. Pestov, S. N. Vdovichev, S. S. Ustavshikov, M. Yu. Levichev, A. V.

- Putilov, P. A. Yunin, A. I. El'kina, N. N. Bukharov and A. M. Klushin, Peculiar superconducting properties of a thin film superconductor-normal metal bilayer with large ratio of resistivities, *Supercond. Sci. Technol.* **31**, 115004 (2018).
- ¹⁹ F. Ando, Y. Miyasaka, T. Li, J. Ishizuka, T. Arakawa, Y. Shiota, T. Moriyama, Y. Yanase, T. Ono, Observation of superconducting diode effect, *Nature* **584**, 373 (2020).
- ²⁰ B. Turini, S. Salimian, M. Carrega, A. Iorio, E. Strambini, F. Giazotto, V. Zannier, L. Sorba, and S. Heun, Josephson Diode Effect in High-Mobility InSb Nanoflags, *Nano Lett.* **22**, 8502 (2022).
- ²¹ B. Pal, A. Chakraborty, P. K. Sivakumar, M. Davydova, A. K. Gopi, A. K. Pandeya, J. A. Krieger, Y. Zhang, M. Date, S. Ju, N. Yuan, N. B. M. Schroter, L. Fu and S. S. P. Parkin, Josephson diode effect from Cooper pair momentum in a topological semimetal, *Nature Phys.* **18**, 1228 (2022).
- ²² A. Sundaresh, J. I. Vayrynen, Y. Lyanda-Geller and L. P. Rokhinson, Diamagnetic mechanism of critical current non-reciprocity in multilayered superconductors, *Nat. Commun.* **14**, 1628 (2023).
- ²³ D. Y. Vodolazov and F. M. Peeters, Superconducting rectifier based on the asymmetric surface barrier effect, *Phys. Rev. B* **72**, 172508 (2005).
- ²⁴ H. M. Greenhouse, Design of Planar Rectangular Micro-electronic Inductors, *IEEE Trans. Parts, Hybrids, Packag.* **10**, 101 (1974).
- ²⁵ S. Ustavshnikov, M. Y. Levichev, I. Y. Pashenkin, N. Gusev, S. Gusev, and D. Y. Vodolazov, Diode Effect in a Superconducting Hybrid Cu/MoN Strip with a Lateral Cut, *J. Exp. Theor. Phys.* **135**, 226 (2022).
- ²⁶ D. Cerbu, V. N. Gladilin, J. Cuppens, J. Fritzsche, J. Tempere, J. T. Devreese, V. V. Moshchalkov, A. V. Silhanek, and J. Van de Vondel, Vortex ratchet induced by controlled edge roughness, *New J. Phys.* **15**, 063022 (2013).
- ²⁷ K. Ilin, D. Henrich, Y. Luck, Y. Liang, and M. Siegel, D. Yu. Vodolazov, Critical current of Nb, NbN, and TaN thin-film bridges with and without geometrical nonuniformities in a magnetic field, *Phys. Rev. B* **89**, 184511 (2014).
- ²⁸ D. Suri, A. Kamra, T. N. G. Meier, M. Kronseder, W. Belzig, Ch. H. Back, and Ch. Strunk, Non-reciprocity of Vortex-limited Critical Current in Conventional Superconducting Micro-bridges, *Appl. Phys. Lett.* **121**, 102601 (2022).
- ²⁹ Y. Hou, F. Nichele, H. Chi, A. Lodesani, Y. Wu, M.F. Ritter, D. Z. Haxell, M. Davydova, S. Ilic, O. Glezakou-Elbert, A. Varambally, F. S. Bergeret, A. Kamra, L. Fu, P. A. Lee, J. S. Moodera, Ubiquitous Superconducting Diode Effect in Superconductor Thin Films, *Phys. Rev. Lett.* **131**, 027001 (2023).
- ³⁰ N. Satchell, P.M. Shepley, M.C. Rosamond, and G. Burnell, Supercurrent diode effect in thin film Nb tracks, *J. of Appl. Phys.* **133**, 203901 (2023).
- ³¹ L. Bauriedl, Ch. Bauml, L. Fuchs, Ch. Baumgartner, N. Paulik, J. M. Bauer, K.-Q. Lin, J. M. Lupton, T. Taniguchi, K. Watanabe, Ch. Strunk, and N. Paradiso, *Nat. Commun.* **13**, 4266 (2022).
- ³² B. L. T. Plourde, D. J. Van Harlingen, D. Yu. Vodolazov, R. Besseling, M. B. S. Hesselberth, and P. H. Kes, Influence of edge barriers on vortex dynamics in thin weak-pinning superconducting strips, *Phys. Rev. B* **64**, 014503 (2001).
- ³³ V.V. Shmidt, The critical current in superconducting films, *Sov. Phys.-JETP* **30**, 1137 (1970).
- ³⁴ R. Kawarazaki, R. Iijima, H. Narita, R. Hisatomi, Y. Shiota, T. Moriyama, and T. Ono, Rectification effect of non-centrosymmetric Nb/V/T superconductor, *Journal of the Magnetics Society of Japan*, 2309R001 (2023).
- ³⁵ D. Margineda, A. Crippa, E. Strambini, Y. Fukaya, M. T. Mercaldo, M. Cuoco, and F. Giazotto, Sign reversal diode effect in superconducting Dayem nanobridges, arXiv:2306.00193.
- ³⁶ S. Ilic and F. S. Bergeret, Theory of the supercurrent diode effect in Rashba superconductors with arbitrary disorder, *Phys. Rev. Lett.* **128**, 177001 (2022).
- ³⁷ H. Bartolf, A. Engel, A. Schilling, K. Ilin, M. Siegel, H.-W. Hubers, and A. Semenov, Current-assisted thermally activated flux liberation in ultrathin nanopatterned NbN superconducting meander structures, *Phys. Rev. B* **81**, 024502 (2010).
- ³⁸ L. N. Bulaevskii, M. J. Graf, C. D. Batista, and V. G. Kogan, Vortex-induced dissipation in narrow current-biased thin-film superconducting strips, *Phys. Rev. B* **83**, 144526 (2011).
- ³⁹ D. Y. Vodolazov, Saddle point states in two-dimensional superconducting films biased near the depairing current, *Phys. Rev. B* **85**, 174507 (2012).
- ⁴⁰ R. Wakatsuki, Yu Saito, S. Hoshino, Y. M. Itahashi, T. Ideue, M. Ezawa, Y. Iwasa, N. Nagaosa, Nonreciprocal charge transport in noncentrosymmetric superconductors, *Sci. Adv.* **3**, e1602390 (2017).
- ⁴¹ F. Qin, W. Shi, T. Ideue, M. Yoshida, A. Zak, R. Tenne, T. Kikitsu, D. Inoue, D. Hashizume, Y. Iwasa, Superconductivity in a chiral nanotube, *Nat. Commun.* **8**, 14465 (2017).
- ⁴² K. Yasuda, H. Yasuda, T. Liang, R. Yoshimi, A. Tsukazaki, K. S. Takahashi, N. Nagaosa, M. Kawasaki, and Y. Tokura, Nonreciprocal charge transport at topological insulator/superconductor interface, *Nat. Commun.* **10**, 2734 (2019).
- ⁴³ K. D. Usadel, Generalized diffusion equation for superconducting alloys, *Phys. Rev. Lett.* **25**, 507 (1970).
- ⁴⁴ M. Yu. Kuprianov and V. F. Lukichev, Influence of boundary transparency on the critical current of "dirty" SS'S structures, *Sov. Phys. JETP* **67**, 1163 (1988).